46th AIAA/ASME/ASCE/AHS/ASC Structures, Structural Dynamics & Materials Conference
18 - 21 April 2005, Austin, Texas

AIAA 2005-2284


# A Comprehensive Model for Multi-Disciplinary Design of a Tiltrotor Configuration

Stanley A. Orr*
*The Boeing Company, Philadelphia, PA, 19142*

*and*

Prabhat Hajela[Ü]
*Rensselaer Polytechnic Institute, Troy, NY, 12180*



**Much of the development of multidisciplinary optimization methodology has been oriented towards fixed wing design. The rotary wing design problem has several key differences from the fixed wing problem that effect the formulation of a multidisciplinary optimization problem. This paper will present a problem formulation for the integrated design of rotor and wing systems of a tiltrotor aircraft. The tiltrotor configuration brings additional complexity to rotorcraft design over the helicopter. A design problem was proposed that consistently places both the wing and rotor in a preliminary design context. The rational for design objectives and constraints is explained. The goal was to exploit the multidisciplinary interactions between the rotor and wing systems, as well as the interactions between the dynamic and aerodynamic design. An additional goal was to develop a problem formulation that is sufficiently complete so as to represent an industrial design situation. The problem was of moderate size and can be easily scaled to large size for both the rotor and the wing. The design problem was formulated to contain a representative set of design variables, objectives, and constraints. The main objective was the combined structural weights of the rotor and wing systems as well as the fuel weight for the cruise mission segment. A random design space survey was used to examine multi-disciplinary and intersystem interactions. State of the art rotorcraft analyses were used in the study. The issue of moderately long CPU times and problem dimensionality pose challenges to optimal search in this design domain. A possible solution strategy for the design problem is the subject of a companion paper.**

## Nomenclature

| | | |
|---|---|---|
| $q$ | = | *dynamic pressure* |
| $b$ | = | *wing span* |
| $e$ | = | *Oswald efficiency factor* |
| $r$ | = | non-dimensional blade station |
| $GW$ | = | aircraft gross weigth |
| $C_{d0}$ | = | zero-lift drag |
| $S$ | = | wing area |
| $t/c$ | = | airfoil thickness ratio |
| $BSFC$ | = | brake specific fuel consumption |
| $Hp_{total}$ | = | total aircraft horsepower |
| $W_{rotor}$ | = | rotor system weight |
| $W_{fuel}$ | = | fuel weight for cruise mission segment |
| $W_{wing}$ | = | wing system weight |
| $\theta_b$ | = | built-in blade twist (pitch) angle |
| $V^Z$ | = | vertical hub shear force |
| $V^{INP}$ | = | resultant in-plane hub shear force |

* Engineer/Scientist, Dynamics, P23-02, Member AIAA.
Ü Professor of Aerospace Engineering, 4226 Walker Lab, Fellow AIAA.

$M^{INP}$ = resultant in-plane hub moment
$\zeta$ = damping ratio
g = constraint
x = design variable
y = design objective

## I. Introduction

The tiltrotor configuration allows vertical take-off and landing but can exploit the efficiency available to a turboprop by tilting the proprotors from vertical, or helicopter mode, to horizontal, or airplane mode. In between is the conversion mode for transition. The tiltrotor configurationís airspeed and altitude envelope encompasses most of both the airplane and helicopter envelopes. Generally, the design requirements are the union of those for airplanes and helicopters with some additions and modifications for the unique aspects of the configuration. The conflicting demands on efficient performance in both flight modes require a compromise design while satisfying all stability constraints applicable to helicopters and airplanes. The proprotor is the main source of vibratory loads that cause vibrations, so it is important the proprotor design does transmit high vibratory hub loads to the wing.

The proprotor aerodynamic design must be a compromise between the rotor required for a helicopter and the propeller required for efficient airplane-mode cruise. An ideal blade twist distribution minimizes induced power; but the ideal for a hovering rotor in helicopter mode is different from high-speed flight in airplane mode. The inflow through the rotor in airplane mode is much higher than through a hovering rotor; the rotor speed in airplane mode is lower to mitigate drag divergence. Rotor speed and inflow differences between airplane and helicopter mode aerodynamics produce different distributions of induced angle of attack so that the blade built-in twist cannot be ideal for both flight regimes. Hover and cruise are axis-symmetric aerodynamically, but the configuration must also fly in edge-wise flight, as in the typical forward flight of a helicopter. Edge-wise flight causes period variations in the aerodynamic environment that place airfoils in severe operating conditions.

As with any rotorcraft, the proprotor blades interact with non-steady aerodynamic forces creating a problem that is inherently multidisciplinary. As the flexible blade deforms under the aerodynamic loading, elastic deflections alter the geometric pitch angle and change the angle of attack, which in turn changes the aerodynamic loading. Rotorcraft analysis generally employs iterative procedures to solve the aerodynamic loading and structural-dynamic responses together. While this coupled solution is critical for the computation of blade loads and vibratory hub forces, it is also required for accurate performance analysis. Even in hover or airplane cruise mode, where the airflow through the rotor is constant around the azimuth, steady blade deformations can be large enough to change the lift distribution and thereby create a strong interaction between the aerodynamic and structural design.

Vibration is one of the most persistent technical problems in rotorcraft. The primary contributors to vibration are the periodic forces that are transmitted from the rotor blades to the fuselage. This is mostly the case in edge-wise flight. Tiltrotor flight is subject to edge-wise flight primarily in the transition from hovering to airplane mode cruise. Aerodynamic design has a big influence on vibratory forces, as well as on blade loads and dynamic stability such as flutter and whirl flutter. The structural design of the blade also impacts vibration, particularly when a near-resonant condition amplifies the dynamic response. The dynamics of the blade impact the strength through the dynamic interactions with aerodynamic loads. The structural design of the blade must meet the strength required to endure high-cycle fatigue loads as well as static loads.

In addition to the conventional modes of instability in rotorcraft such as blade flutter, the large proprotors make the configuration susceptible to a special form of nacelle whirl called whirl flutter. A stiff wing is usually required to mitigate whirl flutter, but this drives the wing thickness up and the cruise performance down. This is the one of the main sources of interdisciplinary interaction involving the rotor and wing systems. As with the rotor, the wing as a structure is required to meet strength requirements for the various loads that the aircraft will experience in service.

This paper will expound a problem formulation for the integrated design of a rotor and wing for a tiltrotor configuration. The objective was to optimize a given preliminary design, and to return structural weight and mission fuel weight to increased payload. Details of the internal rotor and wing structure, wing thickness, and the aerodynamic design of the rotor were design variables. Key analyses will be expounded with attention to how the analyses effect the formulation of the design problem. The details of the objectives, constraints, and design variables will be presented. The body of research in rotorcraft optimization shows an increasing level of sophistication in the problem formulation as well as the use of optimization technology, as exemplified in Refs. 1-5. This work sought to expand these problem formulations and include a more complete representation of multi-disciplinary considerations. Furthermore this problem formulation sought to place the design variables, constraints, and objectives in a context that represented an industrial preliminary design effort.

For this study the conceptual design of the rotor was taken from design study for a replacement for an experimental tiltrotor[6]. Target system weights and payloads were taken from this design. This rotor was an articulated design with a flexure that acts as a flapping and lead-lag spring. This design was soft-in-plane, meaning that the fundamental frequency of the lead-lag motion is lower than the rotor speed at operating rpm. A soft-in-plane rotor is subject to certain modes of instability that are not found in a stiff-in-plane design. An elastomeric damper mitigates these modes of instability and improves some damping for whirl flutter. The fuselage/wing conceptual design was patterned after the experimental tiltrotor design.

As a design moves from a set of requirements to a finished product the level of detail increases. The design process has three main phases: conceptual, at which the general layout of the configuration is defined; preliminary, at which structural details are considered and the aerodynamic design is defined; and detailed, at which the structural details are defined. Certain design features may be borrowed from years of research and development (airfoils, structure concepts, etc.). Design changes that are made late in the design process (detailed design phase) are the most costly and have the least possibility to improve the design significantly. Conceptual design offers the greatest flexibility for design definition, especially in the choice of configuration that bests meets mission requirements. Optimization in the conceptual design phase deals with general sizing, number of blades, layout, engine selection, and so forth. Preliminary design is when structural details and aerodynamic configuration can best be exploited for overall benefit. The problem formulation proposed in this paper was set in the context of preliminary design.

At this stage the structural features of the conceptual layout can be considered as guides to the future detailed design definition; and certain conceptual design characteristic may be considered as problem parameters. For the tiltrotor configuration this includes the wing span and rotor radius. The type of rotor hub has such a strong impact on flying qualities and aircraft dynamics that this choice is made very early. This problem formulation therefore used the following as fixed problem parameters: rotor radius and wing span and planform, number of blades, and hub and blade root geometry.

## II. Analysis

The analytical process ñ computing objectives and constraints from design variables ñ required filtering the design variables through several layers of analyses. Both the wing and the rotor began with low-level internal structural details, but the core rotor and the fuselage/wing analyses required high-level beam properties such as bending stiffness, running weights, inertias, and so forth. Additional post-processing operations were required to convert blade or wing bending and torsion loads into laminate stresses and strength. Other post-processing operations involved computing weights of structural components. Figure 1 shows a high-level view of the analytical process. As an example, the blade modes required blade properties and the wing modes require wing properties for their respective computations. Both were inputs to the whirl flutter analysis, which produces whirl flutter stability and coupled rotor/wing frequencies as outputs.

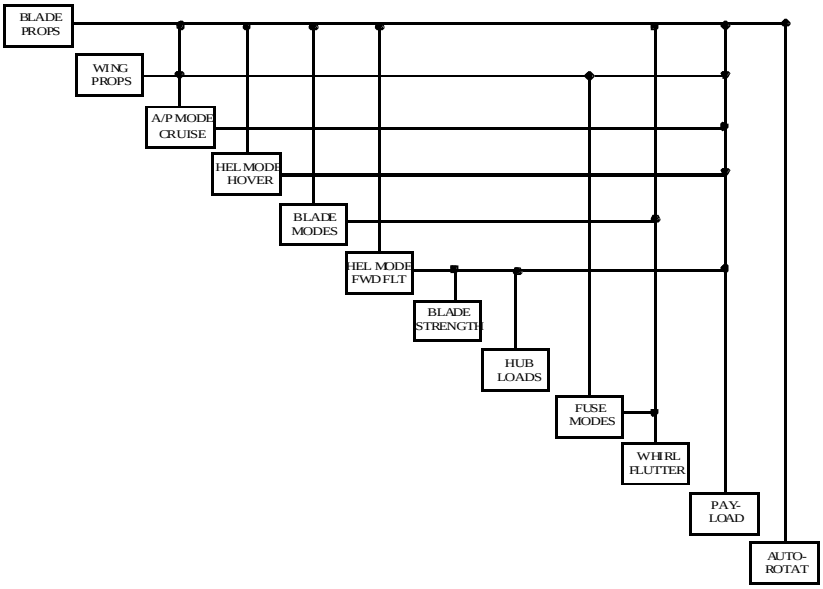


**Figure 1. Overview of Analysis Operations**

Engineering beam theory[7] and classical laminate theory[8] were combined for cross section analysis. Rotor and wing cross sections were represented as combinations of constituent parts. A typical blade cross section is shown in Fig. 2, showing the trailing edge wedge, core, aft fairing, heel, nose block, balance weight, and spar. The inset exemplifies how each constituent is a built-up laminate. Laminate analysis for each constituent part provided effective engineering young modulus, shear modulus, and densities, which were computed using classical laminate theory. Beam properties for the finite element models were computed by modulus or density-weighted cross section integrals for bending stiffness, running weight, inertia, and so forth. Contributions from each constituent were integrated exactly, and then summed. Cross sections were modeled as multi-cell structures for torsion stiffness, where modulus-weighted contour integrals were integrated exactly for each constituent part and then summed as for the bending properties. This process mapped the basic properties of the cross section, such as the numbers of materials of various plies, as well as gross features of the blade geometry such as chord length, thickness and heel placement, from low-level details (design variables in this case) to high-level beam properties used by the core analysis processes. Note also that this process also provided data for computing system weights. This combination

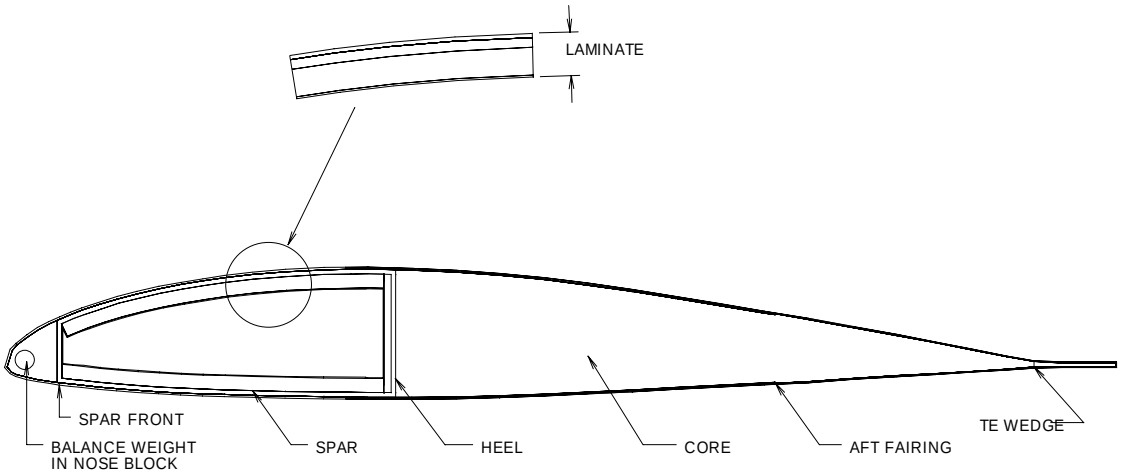


**Figure 2. Blade Cross Section**

of simple theories provided a beam section analysis that that could efficiently convert structural details into beam properties, which was important for use in optimization. A more sophisticated approach was not deemed sufficiently simple or necessary for this context. Beam properties were required by the rotor and coupled rotor/fuselage analysis that provided most of the system responses for objectives and constraints.

Rotor performance, loads, blade modes, and flutter stability were computed using a dedicated analysis tool, 2GCHAS (Second Generation Comprehensive Helicopter Analysis System[9,10]). 2GCHAS is a finite element based system that combines nonlinear beam elements with high fidelity aerodynamic modeling, including airfoil lookup tables, unsteady aerodynamics, dynamic stall, and vortex filament wakes for computing the non-uniform distribution of induced flow through the rotor disk. This level of modeling sophistication is required for preliminary design.

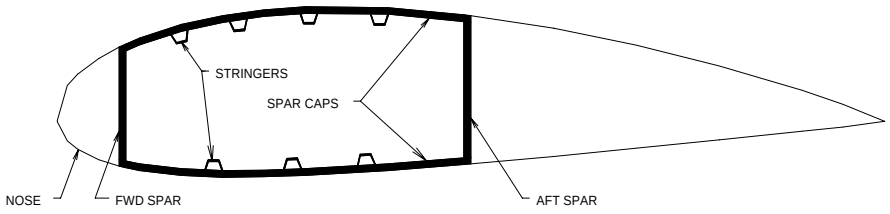


**Figure 3. Wing Cross Section**

Whirl flutter damping and rotor/wing coupled frequencies are computed simultaneously in the whirl flutter analysis using the program PASTA[11], which employs modal analysis of the rotor and wing systems. The wing/fuselage system was represented by the normal modes computed in 2GCHAS by taking the frequencies, generalized masses, and modal motion at the rotor hub. The rotor modes are the fundamental modes in the flap and lead-lag directions, which for an articulated rotor are defined by the span-wise location of the hinges, which in this case are coincident, and the frequencies of these modes, which were computed in the 2GCHAS natural frequency analysis.

The rotor analytical model consisted of non-linear finite elements representing the blade, flexure, CF-beams, pitch arm, and pitch link, Fig. 4. The coincident flap-lag-pitch bearing and outboard uniball bearing were included in the model. The lag damper, which is stroked by relative motion between the blade and flexure tip, was modeled as a linear spring and damper. Likewise the fuselage/wing analytical model employed the same finite elements as the rotor, Fig. 5. The geometry and baseline weights were taken from Refs. 12 and 13.

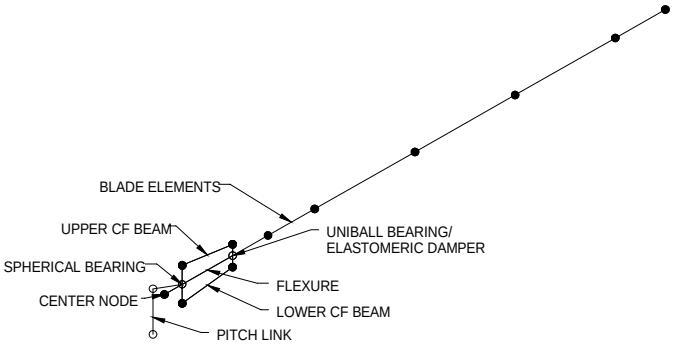


**Figure 4. Rotor Finite-Element Model**

Additional post-processing operations computed the strength for each laminate in the blade and wing cross sections from the applied loads. For the rotor, the applied loads were taken as the vibratory blade bending and torsion moments in high-speed edgewise flight, computed in 2GCHAS. Wing loads were taken as the worst of three cases described in Ref. 14. In the case the transition pull-up was the most severe and was used exclusively for the wing external loading.

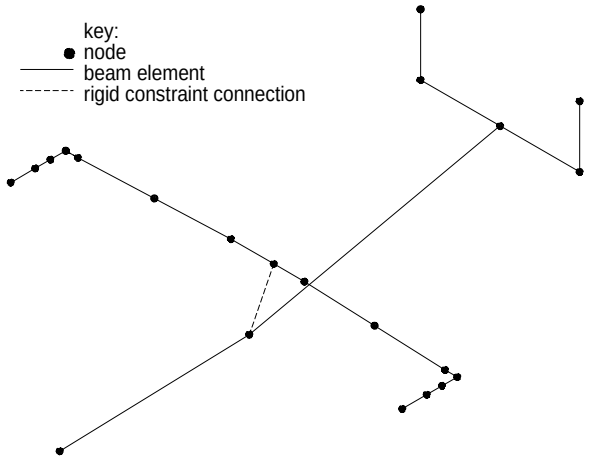


**Figure 5. Fuselage/Wing Finite-Element Model**

The same laminate analysis that was used to obtain engineering constants and densities for the weighted cross section integral properties was also used for post-processing the blade and wing internal bending and torsion moments. Bending moments were converted to equivalent laminate loads by equating the strains at the upper and lower surface of each laminate to the combined strains from beam-wise and chord-wise bending. The shear flow per unit applied moment was known from the torsion stiffness calculation; therefore the laminate shear load was just the actual cross section torsion times the local shear flow. This provided three laminate loads for the cross section from the three beam internal moments, as shown in Fig. 6, which shows the conversion to laminate loads for the upper spar. Additional simple computations processes were required to get system weights from cross section running weight. The core analytical processes were:

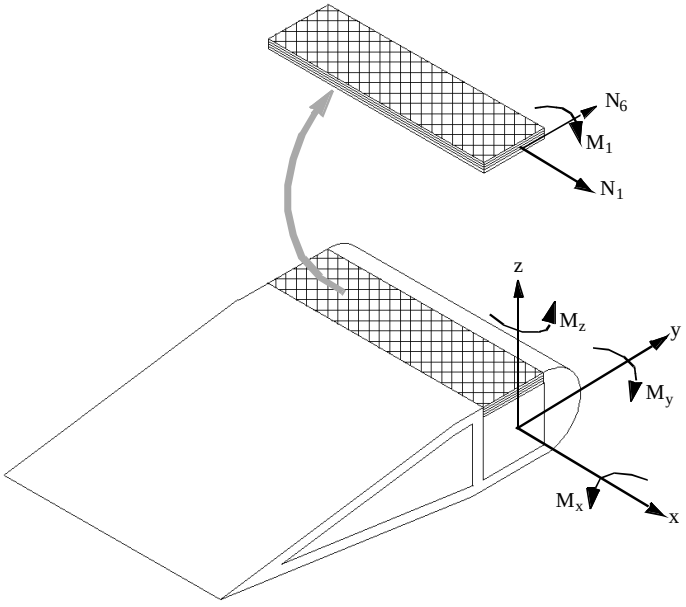


**Figure 6. Laminate Loads from Cross Section Loads**

- section analysis: conversion of plies and cross section geometry into beam properties
- weight analysis: blade inertias and weights
- 2GCHAS: single isolated-blade frequencies and modes
- 2GCHAS: single isolated-blade performance and blade flutter in airplane mode at airplane mode cruise rpm at 275 knots
- 2GCHAS: single isolated-blade performance and blade flutter in helicopter mode hover

- 2GCHAS: single isolated-blade vibratory blade loads and hub reactions in helicopter mode forward flight at 120 knots
- 2GCHAS: fuselage/wing frequencies and modes
- PASTA: whirl flutter analysis at 375 knots and coupled rotor/fuselage/wing frequencies
- section analysis: laminate strength

Airplane mode performance was the connection from the wing thickness to rotor performance. Wing thickness increases drag, and this was accounted for by computing the thrust required in airplane mode cruise as a function of wing thickness. Aircraft parasite drag and the induced drag were taken as constant for 275 knots and 13000 pound gross weight. The profile drag was taken from the zero-lift drag coefficients of the NACA series 44XX airfoils as a curve fit function of wing thickness. The drag that must be overcome by total rotor thrust was determined by Eq. (1)

$$Drag = q \cdot f_e + \frac{GW^2}{q \cdot b \cdot \pi \cdot e} + q \cdot S \cdot C_{d0}(t/c) \tag{1}$$

Fuel weight for cruise was determined by assuming a 3.5 hour cruise mission segment and brake specific fuel consumption (BSFC) of 0.5 lb/hour/Hp, Eq. (2). BSFC was held constant in this formulation; though a variable BSFC could be included as a function of engine speed.

$$W_{fuel} = BSFC \cdot (3.5) \cdot Hp_{total} \tag{2}$$

Aerodynamic performance of the rotor was essential to the objective function valuations. Rotor analysis typically uses so-called C81 format airfoil tables that provide a complete map of two dimensional airfoil coefficients verses Mach number from zero to one and angle of attack from -180 to 180 degrees. This model employed a set of airfoils that were specified at select span-wise location on the blade. Two aspects of blade modeling in 2GCHAS are relevant: The blade is discretized into aerodynamic bays, which should be somewhat uniform in size. And, each airfoil is assigned to a region of the blade so that any bay center that is within a particular region will be assigned the aerodynamic properties of the corresponding airfoil. This modeling assumption is built into the 2GCHAS modeling approach and requires that an assumption be made when the actual airfoils blend from one to the next. It will be seen in the following discussion of blade thickness that the ranges of application for two of the airfoils were design variables. Given a fixed aerodynamic bay geometry, the range of application for the airfoils as variables would only produce a change to the aerodynamic model if the range moved across the center of the next aerodynamic bay. Otherwise no change would be apparent to the analytical model. This limitation effectively caused the airfoil placement design variables to be discrete. It can be seen that the analytical modeling approach can influence the choice of search type ñ gradient or stochastic.

The analysis models were capable of providing a level of fidelity that is appropriate for preliminary design, especially for performance, loads, and strength. The analytical models were also capable for providing a rich set of design variables as well as a representative set of objectives and constraints. Analysis run time was therefore representative so that the potential use of surrogate models could be evaluated, especially by way of accuracy verses run time.

## III. Design Variables

Design variables were selected to be consistent with the preliminary design phase in the level of detail. In general, design variables included the aerodynamic configuration of the rotor blades, the thickness of the wing, and the rotor speed. The internal details of the blade and wing structures were included. The numbers of plies in the cross section laminates were the primary structural variables. The number and cross section area of stringers were used for the wing. The aerodynamic design coupled the structural design primarily through blade and wing thickness, as well as the blade. Spar placement was variable for both the blade and wing.

While early rotor blades required a simple rectangular planform for manufacturing, the use of composites in blade construction has allowed for flexibility in the blade design. Several planform schemes were considered for a tiltrotor replacement blade including a design that reduced the chord size in multiple tapered steps[15]. Some researchers have used an arbitrary polynomial to define the blade chord distribution in which the polynomial coefficients were design variables[16]. The current formulation employed a similar approach, but in this case only the tip chord was varied ñ one design variable. Current production tiltrotors employ a straight tapered planform which allows both the structural simplicity of a straight spar and the aerodynamic benefit of reduced tip chord. A lower bound on tip chord was used as an implicit constraint on minimum blade area for maneuverability. Advanced tip shapes would be more critical for a high-speed tiltrotor.

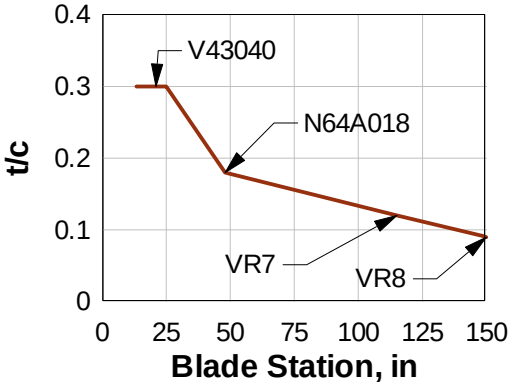


**Figure 7. Baseline Airfoil Distribution**

The aerodynamic environment of the rotor is very demanding in that the range of angle of attack and Mach number varies dramatically with each revolution of the rotor during edgewise flight. The compromise between hover and cruise demands a trade-off between high maximum lift coefficient and high drag divergence Mach number. Airfoils for application in rotorcraft have been carefully researched[17]. The use of inversely designed[18] or ì rubberî airfoils in optimization would provide a desirable level of flexibility, but rotor analysis requires a complete set of airfoil data from low to high Mach number and from -180 to 180 degrees angle of attack. The computation would be too expensive for this application and the characterization might not be sufficiently reliable for preliminary design. Therefore this formulation used a pre-selected set of airfoils, which have been used in a previous tiltrotor blade design[13]. Figure 7 shows the baseline configuration of airfoils: 30% airfoil that covers the rotor hub, 18%, 12%, and 9% airfoil that defines the tip.

Blade thickness is significant both to the aerodynamic design and the structural design; the blade structure is constrained by the blade outer mold line. Therefore the placement of the airfoils can impact the structural performance through stiffness, strength, and weight, as well as the aerodynamic performance. This is one of the main aspects that make this a multi-disciplinary design problem. The distribution of thickness in the current problem was varied during optimal search by variation in the span-wise placement of the 12% and 18% airfoils ñ two design variables. Thickness was prescribed by the variable placement of these airfoils along with select root and tip airfoils.

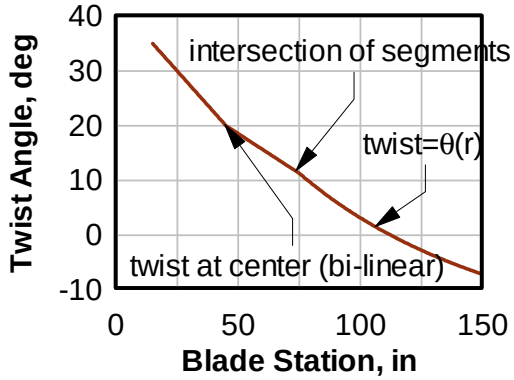


**Figure 8. Baseline Twist Distribution**

Blade built-in twist was defined as a two-stage function. The concept of ideal twist was used in the definition of the outboard stage. Ideal twist is a distribution of the blade twist angle that, by alignment of the local blade section induced angle of attack, allows minimum induced power. Note that because of the different rotor speeds and inflow, the hover and cruise ideal twist are very different. The design variable $u_1$ in Eq. (1) was used to express the ideal twist distribution for hover, cruise, or in between. The inboard twist segment was a bi-linear function defined by the twist at the center of the bilinear segment and the location of the intersection of the inboard and outboard stages. Fig. 8 shows how the built-in twist was defined by these three design variables. The flexibility of this approach was in the ability to capture ideal twist for hover, cruise, or in between, as well as to reproduce closely the shape of the baseline and optimal twist distributions of Ref. 19. The ranges for the twist variables also allowed the design to move from hover and cruise ideal twist.

$$\theta_b(r) = \tan^{-1}\left(\frac{u_1}{r}\right) - \tan^{-1}\left(\frac{u_1}{3/4}\right) \tag{3}$$

The importance of the rotor speed selection was noted above. In hover the rotor speeds are high to produce high dynamic pressures. In airplane-mode cruise, however, the rotor speed must be reduced to avoid drag divergence. A range of airplane mode rotor speeds was selected as another design variable and encompassed the range of rotor speeds of two different tiltrotor blade designs, Refs. 20 and 21.

Structural design variables such as numbers or angles of plies are low-level details. Other formulations have used low-level details, but typically with a box-beam idealization as in Ref. 22. High-level beam properties have been used directly as design variables as in Ref. 23. High-level properties provide at least eight design variables for each cross section: flap bending stiffness, chord bending stiffness, torsion stiffness, running weight, flap-wise inertia, chord-wise inertia, center-of-gravity offset, and neutral axis offset. Note that cross section properties cannot really be varied independently, especially when the outer mold line is constrained by the aerodynamic shape. Beam section properties are interrelated; for example, increasing bending stiffness may require more structural material, which increases running weight. Therefore the use of high level beam properties requires a scheme to constrain the relationships of the beam properties. The interrelations among beam properties are further constrained by the internal configuration. Blade structural typically comprise of a D-shaped spar with a solid nose block and an aft fairing with honeycomb core as described above. The use of low-level details in this work was chosen to manage these interrelations automatically. Furthermore this approach of pre-selecting an internal configuration introduced an implicit constraint on design for manufacturability.

Other research combined low-level and high-level structural optimization in a hierarchical decomposition approach as in Ref. 24, and was shown to be an effective approach. The upper-level optimization maintained high-level beam properties as design variables while the lower-level problem attempted to find low-level details that allow the beam properties to be matched. This approach adds complexity unless the number of low-level details is greater than the number of high-level beam properties, in which case the high-level problem size would be smaller. The cross section definition of this study had the potential to allow at least five to ten parameters that define the cross sections to be used as design variables (some would apply to all cross sections, such as the spar chord-wise location). This work used two for each of five the rotor blade cross sections: the number of spar unidirectional plies and the number of spar cross plies (angled laminates). The spar chord-wise placement was an additional design variable applied to the outer four stations for a total of 11 design variables for the blade structure. The station 31 cross section was a transition from the root hub connection to the main blade sections; therefore the spar location was not included in the spar placement design variable. Fig. 9 shows the span-wise locations of these cross sections superimposed on the blade planform.

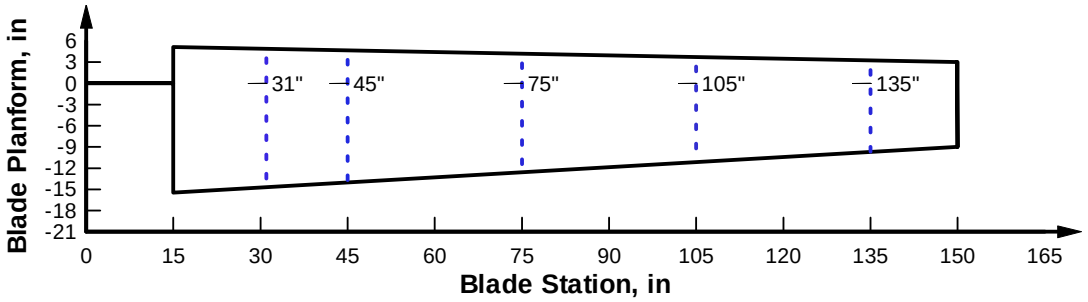


**Figure 9. Blade Stations for Cross Section Analysis**

Details of three wing cross sections were likewise used as design variables: the numbers of spar unidirectional and cross plies (forward and aft spars), the numbers of spar cap unidirectional and cross plies (same for top and bottom), the numbers of spar unidirectional and cross plies in the nose, the angle of all cross plies, the number and cross section area of stringers (one set of variables for the entire wing), and the wing thickness ratio ñ 32 design variables.

Finally, the wing thickness ranged from 15 percent to 24 percent. This set of design variables provided 18 associated with the rotor and 33 associated with the wing. Other details that define each cross section were retained as fixed problem parameters. Two approaches to scaling the problem size are easily available: add more blade or wing stations, or convert problem parameters to design variables. As defined, the current problem allows span-wise space for transition from one blade or wing section to the next. If more blade or wing stations are used, then additional constraints may be required to control the ply drop-off or build-up along the span.

## IV. Design Objectives and Constraints

### A. Objective Functions

The primary global objective was to minimize weight that can be returned to increase payload. The sum of system weights of the rotor and wing, and fuel weight for the cruise mission segment were the main objectives for minimization. Additional objectives were to minimize vibratory hub loads from the rotor, which act on the fuselage and cause vibrations. These were the 3-per-rev and 6-per-rev vertical hub force, resultant in-plane hub force, and resultant in-plane hub moment. The individual objectives are shown in Eq. (4).

$$\begin{aligned} &\text{Minimize:} \\ &y_1 = W_{rotor} + W_{fuel} + W_{wing} \\ &y_2 = V_{3P}^{Z} \\ &y_3 = V_{6P}^{Z} \\ &y_4 = V_{3P}^{INP} \\ &y_5 = V_{6P}^{INP} \\ &y_6 = M_{3P}^{INP} \\ &y_7 = M_{6P}^{INP} \end{aligned} \tag{4}$$

A multi-objective approach was sought for this problem. It is desirable in any optimization to formulate objectives that are relevant to meaningful system performance. One measure of aircraft performance is productivity, which is the product of the useful load and the block speed. In this problem the cruise speed was set at 275 knots; therefore the useful load, or payload, was of interest. It was appropriate therefore to add the weights of the rotor, fuel, and wing in the first objective $y_1$, but the hub loads objectives required special treatment.

Solving vibration problems may require up to five percent of the empty weight[25]. This weight is often in the form of structural tuning to remove structural frequencies from proximity to key excitation frequencies, primarily from the rotor. It was therefore proposed to credit the vibratory hub forces as weight. The desirability function approach was used to map the vibratory hub loads from zero to one. This approach combined desirability functions into one measure by taking the geometric mean of each. Equation (5) shows the mapping of the hub loads $V_i$ to desirability functions $d_i$ through arbitrarily-defined upper and lower bounds $V_{UBi}$ and $V_{LBi}$.

$$\begin{aligned} D &= \left( \prod_{1}^{6} d_i \right)^{1/6} \\ d_i &= \frac{V_i - V_{LBi}}{V_{UBi} - V_{LBi}} \end{aligned} \tag{5}$$

The geometric mean $D$ of the hub loads desirability functions provided a way to include the hub loads objectives with the weight objectives by scaling the hub loads desirability by a fraction of empty weight as shown in Eq. (6). The nominal value was selected as 3.5 percent of the empty weight. The maximum value of D is one, so the full factor of when is added to the objective only when all hub loads are at their highest levels.

$$\begin{aligned} y &= W_{rotor} + W_{fuel} + W_{wing} + K \cdot D \\ K &= 318.5 \end{aligned} \tag{6}$$

### B. Aerodynamic Constraints

While the main tiltrotor mission segment is cruise, the tiltrotor is also a vertical takeoff aircraft. The ability to hover must be retained, though hover efficiency is not as critical. Cruise performance is a trade-off with hover performance, so a hover power constraint was employed to keep the hover power below a baseline maximum. It was

noted that the airplane mode rpm is lower than the helicopter mode rpm to avoid drag divergence. Torque is inversely proportional to rotor speed, which in this problem formulation was variable. A torque constraint was included so that if the optimal search lowered the rotor speed, the torque would not exceed a maximum value. This constraint was an alternative to including the drive train system weight in the primary objective

$$\text{Subject To:}$$
$$g_1 = \frac{P_{hover}}{P_{baseline}} - 1 \le 0 \tag{7}$$
$$g_1 = \frac{Q}{Q_{\max}} - 1 \le 0$$

**C. Rotor Structural Constraints**

Helicopter mode forward flight is an edgewise flight mode that produces vibratory loads in the rotor. High-speed level flight (120 knots helicopter mode) was used as the high-cycle fatigue case. Fatigue strength was constrained in the pitch links and in five blade stations (the same stations at which cross section design variables were employed). Vibratory blade bending moments were used to calculate strength at each cross section, as described above. Reserve factors (or strength ratios), *RF*, for each ply in each laminate were used in a cumulative constraint (K-S function[26]), one for each cross section. These were compared to a minimum reserve factor, $RM_{min}$. The parameter $\rho$ dictates how closely the cumulative constraint follows the intersections of the individual constraints. This approach condensed the individual constraints on the strength of each ply in each laminate into one constraint for each cross section.

$$\text{Subject To:}$$
$$g_3 = \frac{PLL}{PLL_{\max}} - 1 \le 0$$
$$g_i = 1 - \frac{RF_i}{RF_{\min}} \le 0 \qquad i = 1 \ldots N_{plies} \tag{8}$$
$$g_n = \frac{1}{\rho} \cdot \ln\left(\sum_i \exp(\rho \cdot g_i)\right) \qquad n = 4 \ldots 8$$

Because the blade structural properties changed during the optimal search, blade flutter constraints were included to prevent the search from generating an unstable design. Blade flutter is similar to wing flutter where damping is generally reduced when the center of gravity moves aft.

$$\text{Subject To:}$$
$$g_{9,10} = 1 - \frac{\zeta_{flutter}}{\zeta_{\min}} \le 0 \tag{9}$$

Autorotation is a non-powered state where the rotor continues to rotate as the up-wash through the descending rotor pushes the blades to continue rotation. A safe landing can be achieved by extracting kinetic energy from the spinning rotor to slow the descent before touchdown. The optimization objective attempted to lower the blade weight. If a rotor becomes too light however, there will not be sufficient rotary inertia to allow for a safe autorotation flare; therefore the blade inertia was constrained to be higher than a minimum by way of the autorotation index *AI*, which is the ratio of the rotary kinetic energy stored in the spinning rotor to the disk loading (nominal thrust divided by rotor area) times aircraft weight. The *AI* is a benchmark for estimating the ability of a rotorcraft to perform a safe autorotation landing.

$$\text{Subject To}:$$

$$g_{11} = 1 - \frac{AI}{AI_{\min}} \le 0 \tag{10}$$

### D. Coupled Rotor/Fuselage/Wing Constraints

Two main sources of rotor to wing interaction are through whirl flutter stability and coupled frequencies. Coupled rotor/wing frequencies must not intrude into avoid bands centered at the respective helicopter and airplane mode rotor frequencies, or integer multiples of the rotor speed times the number of blades. Frequency separation avoids a resonant condition that can increase vibrations. In this problem (with a low-fidelity finite element model) the key system natural frequencies were below 3-per-rev, so only 1-per-rev frequency separation constraints were used. Weight, stiffness, and shape variations from blade to blade cause variations in blade track and balance, which causes 1-per-rev vibrations. Frequency separation requirements were two-sided. A second order constraint was formulated so that the normalized value was one when the structural frequency equals the avoid frequency, zero at the boundaries of the avoid band, and negative outside the avoid band. The constraint is demonstrated in Fig. 10, where the avoid frequency is 30 and the avoid band ranges from 28 to 32.

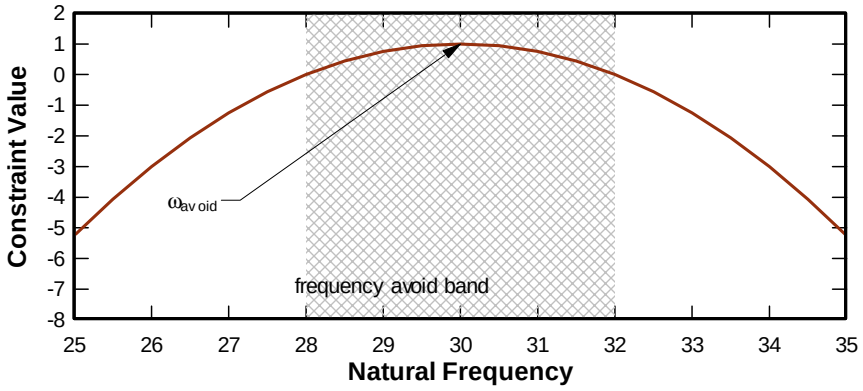


**Figure 10. Second Order Frequency Constraint**

These second order constraints were combined with a cumulative constraint function as were the strength constraints, Eq. (11).

$$\begin{aligned}
&\text{Subject To}:\\
&g(\varpi, \varpi_{hover}, \sigma)_i \le 0 \quad i = 1 \ldots N_{\text{mod es}}\\
&g_{12} = \frac{1}{\rho} \cdot \ln\left(\sum_i \exp(\rho \cdot g_i)\right)\\
&g(\varpi, \varpi_{cruise}, \sigma)_i \le 0 \quad i = 1 \ldots N_{\text{mod es}}\\
&g_{13} = \frac{1}{\rho} \cdot \ln\left(\sum_i \exp(\rho \cdot g_i)\right)
\end{aligned} \tag{11}$$

While wing stiffness is required to tune the structural frequencies, it is also required to mitigate whirl flutter instability. Whirl flutter instability may involve any coupled rotor/wing mode, so all coupled modes were checked. This was accomplished in the same manner as the blade strength constraints, using the cumulative constraint function effectively to find the mode with the lowest damping.

$$\text{Subject To:}$$
$$g_i = -\zeta_{whirl\ i} \le 0 \quad i = 1 \ldots N_{\text{mod es}}$$
$$g_{14} = \frac{1}{\rho} \cdot \ln\left(\sum_i \exp(\rho \cdot g_i)\right) \tag{12}$$

**E. Wing Structural Constraints**

The wing is also subject to loading that requires the strength to be constrained during optimal search. The jump take-off condition provided the primary static load case for wing strength analysis. As with the rotor, the reserve factor for each ply was constrained to be greater than the minimum reserve factor, $RF_{min}$. Wing skin panel buckling was also constrained by comparing the skin panel axial load to the critical load, which is especially important because the number of stringers is a design variable, and the panel width changes with the stringer spacing.

$$\text{Subject To:}$$
$$g_i = 1 - \frac{RF_i}{RF_{\min}} \le 0 \quad i = 1 \ldots N_{plies}$$
$$g_n = \frac{1}{\rho} \cdot \ln\left(\sum_i \exp(\rho \cdot g_i)\right) \quad n = 15 \ldots 17 \tag{4}$$
$$g_n = \frac{N}{N_{critical}} - 1 \le 0 \quad n = 18 \ldots 20$$

## V. Subsystem and Multidisciplinary Interactions

The proposed design problem exhibited interactions between the design of the rotor and wing systems. It was noted that rotorcraft analysis is inherently multidisciplinary. This section will focus on establishing the previously-mentioned multidisciplinary and inter-system interactions. A complete review of main effects was presented in Ref. 27, which includes a survey of intra-disciplinary effects as well.

A survey of the design space was performed using 1000 executions of the complete set of objectives and constraints using a uniform random distribution of design variables. The primary tool for investigating effects on responses from the design variables was scatter plots with superimposed second-order trend curves. While this tool provided excellent insight, additional techniques were required to assist engineering judgment. Single-point finite difference calculations were occasionally employed to compute sensitivities. A statistical technique was also used. Regression analysis includes a statistical measure of the significance of regression parameters ñ the P-value[28]. The P-value estimates the probability that a regression parameter is actually zero. This information is especially helpful when comparing regression coefficients, which are dimensional quantities that might be small in magnitude but significant nonetheless.

Blade aerodynamic design effects blade loads, so the effect on blade structural response is not unexpected. Figure 11 shows four aerodynamic design variables and their effects on hub loads, pitch link loads, and blade strength. It can be seen that the aerodynamic design alone can produce significant reductions in hub loads. Note that in conventional design practice the aerodynamic design is, for the most part, separate from structural considerations, so it is up the blade design team to lower vibratory hub loads through the structural dynamics alone. Pitch link loads were also affected significantly; this interaction is well known. The effect on blade strength from the span-wise airfoil placement is a manifestation blade thickness. The blade is thicker overall when the 18% airfoil placement moves outboard and thinner when it moves inboard, and the bending stiffness increases and decreases accordingly. This change in stiffness changes the blade dynamics and therefore the response to airloads; but the stiffness has a big effect on blade strains, and hence the strong effect on blade strength. Note that because of the potential to change airloads, blade dynamics, and strain, it is difficult to establish a direct cause of the effect.

The effect on blade aerodynamic performance from blade structural design is not as clear. Blade deformations under aerodynamic loads effectively create a different twist distribution that in turn changes the aerodynamic loading. The elastic deformation can be several degrees at the blade tip. The random survey showed that within the range of design structural design variables this effect is moderate to small. Figure 12 shows the random survey data

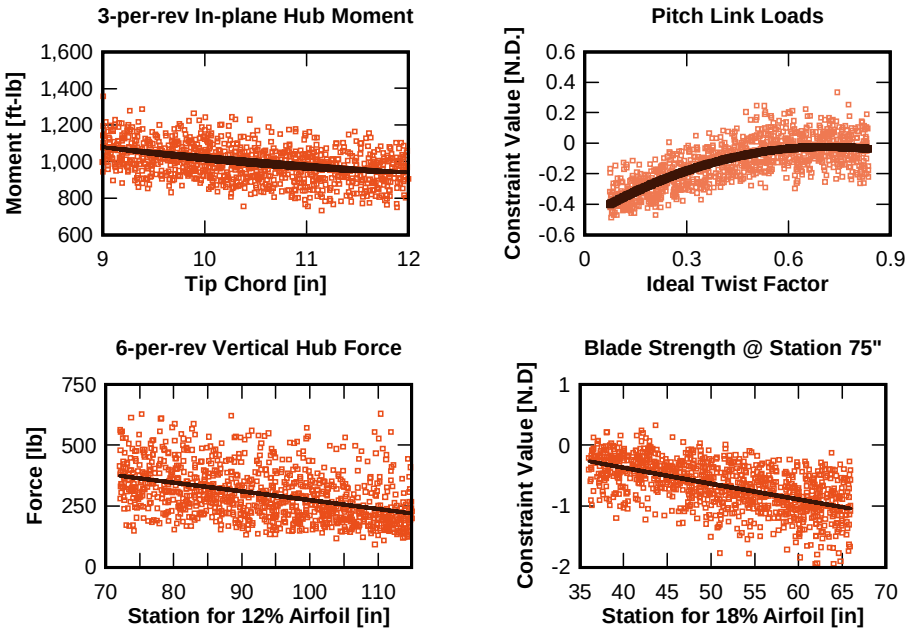


**Figure 11. Effects of Blade Aerodynamic Design on Dynamic and Structural Responses**

for cruise power verses the sum of the number of blade plies variables, which can be used as a rough measure of blade stiffness. No trend can be discerned easily from the survey data, but the trend curve moves slightly downward. The P-value test showed that the regression coefficient was significant, with only 1.5% probability that the coefficient was actually zero. Therefore the effect on performance from the blade structural design was characterized as moderate from the standpoint of establishing interdisciplinary interactions.

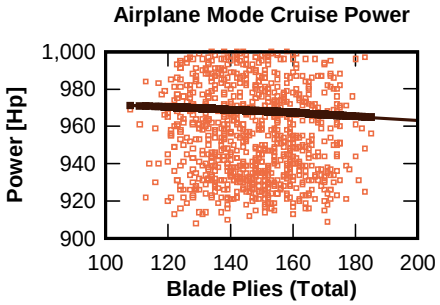


**Figure 12. Effects of Blade Structural Design on Aerodynamic Performance**

The primary influence from the rotor on the wing design is through the rotor speed, which was a design variable. The rotor speed design variable created a moving target for the frequency separation constraint because the coupled natural frequencies were constrained to avoid resonance at the rotor speed frequency The influence on coupled frequencies was embedded directly into the constraint. As for whirl flutter, increased rotor speed creates higher dynamic forces and aerodynamic forces from the higher dynamic pressures; both can aggravate whirl flutter stability. Blade chord also influences the wing design problem through an effect on whirl flutter damping. For the baseline design a change in tip chord from 12 inches to 9 inches raised the critical damping ratio of the critical (lowest damping) mode almost 1/2%. Rotor mass and inertia also influence whirl flutter stability. A lighter rotor has lower flapping inertia; a 23% reduction in flapping inertia (isolated change) raised the critical damping ratio of the critical mode almost 1%. An additional, though smaller, influence from the rotor on the wing comes from the weight of the rotor system itself. The location of the rotors, being placed at the wing tips, is best for influencing the frequencies of the wing bending modes. These affects are demonstrated in Fig. 13.

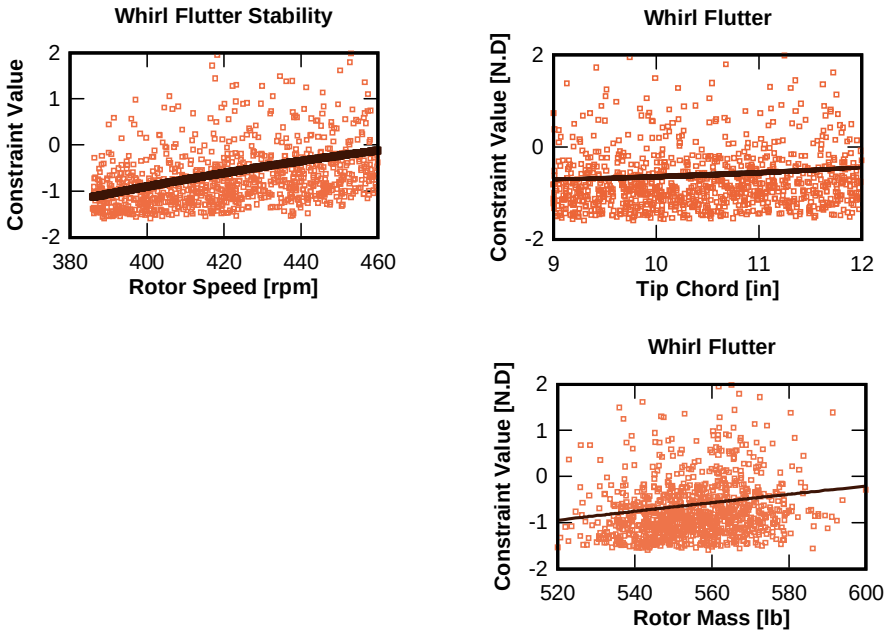


**Figure 13. Effects of Rotor Design on Whirl Flutter**

Finally, influence from the wing design on the rotor design comes from the effect of wing thickness on total aircraft drag as previously discussed. Increased aircraft drag from a thicker wing must be overcome by additional rotor thrust, which requires more horsepower and more fuel for a prescribed cruise mission segment. Given the range of wing thickness in the proposed problem, from 15% to 24%, first order rotor performance analysis suggests

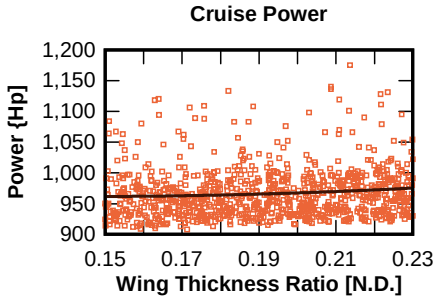


**Figure 14. Effect of Wing Thickness Rotor Aerodynamic Performance**

an increase of 14 horsepower per rotor, or 25 pounds of fuel for a 1.5 hour cruise segment. Linear trend lines of the survey data show ranges of 18 horsepower and 31 pounds of fuel for the given range of wing thickness. A thinner wing is regarded as desirable for any tiltrotor, but especially so for a high-speed tiltrotor as noted in Ref. 29. The cruise speed in this design problem was only 275 knots, which is in the range of the typical tiltrotor cruise speeds; therefore the effect on performance was only moderate as seen in Fig. 14. Note that in an optimal search the wing thickness will be driven down under the influence of structural weight and cruise fuel weight objectives but whirl flutter stability will push the wing thickness up to maintain structural stiffness.

## VI. Conclusions

An integrated tiltrotor preliminary design problem has been formulated so that optimization strategies can be evaluated. The problem design variables, objectives, and constraints have a fairly complete representation from key disciplines: aerodynamic performance, loads, strength, and aeroelastic stability. The analysis is such that the number of design variables can scale to a large-size problem, though the current problem contained 18 design variables associated with the rotor and 33 associated with the wing. Disciplinary interactions were demonstrated between the aerodynamic and structural design of the rotor. Inter-system interactions were also demonstrated between the wing

and rotor systems through the effects of the rotor design on whirl flutter stability and through the influence of wing thickness on rotor performance.

The balance of competing influences is the challenge for a multi-disciplinary design effort. Multi-disciplinary and inter-system interactions must be managed during an optimal search, which may make decomposition difficult. Problem size was big enough, and run time was long enough to consider alternate strategies such as surrogates and decomposition. Both were part of a companion paper on the solution to this challenging problem, Ref. 30.

## References


[1] Walsh, J., Tarzanin, F. J., Young, D. K., ìOptimization Issues with Complex Rotorcraft Comprehensive Analysis,î AIAA Paper 98-4889, 7th AIAA/USAF/NASA/ISSMO Symposium on Multidisciplinary Analysis and Optimization, St. Louis, Missouri, September, 1998.

[2] Ganguli, G., Chopra, I., ìAeroelastic Optimization of an Advanced Geometry Helicopter Rotor,î Presented at 33rd AIAA/ASME/ASCE/AHS/ASC Structures, Structural Dynamics, and Material Conference, Dallas, Texas, 1992.

[3] Peters, D., Cheng, Y., ìOptimization of Rotor Blades for Combined Structural, Performance, and Aeroelastic Characteristics,î Second NASA/Air Force Symposium on Recent Experiences in Multidisciplinary Analysis and Optimization, NASA Langley Research Center, September, 1988.

[4] Liu, John, Paisley, David J., Hirsh, J., ìTiltrotor Aerodynamic Blade Design by Numerical Optimization Method,î Proceedings of the American Helicopter Society 46th Annual Forum, Washington DC, May 21-23, 1990.

[5] Chattopadhyay, A., McCarthy, T. R., ìA Coupled Rotor/Wing Optimization Procedure for High Speed Tilt-Rotor Aircraft,î Proceedings of the American Helicopter 51st Annual Forum, Fort Worth, TX, 1996.

[6] Alexander, H., Smith, K., McVeigh, M., Dixon, P., McManus, B., ìPreliminary Design Study of Advanced Composite Blade and Hub and Nonmechanical Control System for the Tilt-Rotor Aircraft Volume I - Engineering Studies,î NASA-CR-152336-1, November, 1979.

[7] Megson, T. H. G., *Aircraft Structures for Engineering Students*, Edward Arnold, London, 1972.

[8] Tsai, S. W., Hahn, H. T., *Introduction to Composite Materials*, Technomic, Lancaster, PA, 1980.

[9] Anon. 2GCHAS Userís Manual, Vols. I and II, USAATCOM TM 93-A-002, August 1995.

[10] Anon. 2GCHAS Theory Manual, USAATCOM TM 93-A-004, August 1995.

[11] Proprotor Aeroelastic Stability Analysis Version. 4.4 (PASTA), Ray Kvaternik, 2002.

[12] Magee, J., Alexander, H., ìA Hingeless Rotor XV-15 Design Integration Feasibility Study, Volume I and II,î NASA-CR-152310, March 1978.

[13] Acree, C., ìAn Improved CAMRAD Model for Aeroelastic Stability Analysis of the XV-15 With Advanced Technology Blades,î NASA TM 4448, March, 1993.

[14] Peyran, R. J., Rand, O., ìThe Effect of Design Requirements on Conceptual Tiltrotor Design,î Presented at The American Helicopter Society 55th Annual Forum, Montreal, Quebec, 1999.

[15] Magee, J., Alexander, H., ìA Hingeless Rotor XV-15 Design Integration Feasibility Study, Volume I and II,î NASA-CR-152310, March 1978.

[16] Chattopadhyay, A, Narayan, J. R., ìOptimum Design of High Speed Prop-Rotors Using a Multi-disciplinary Approach,î Proceedings of the American Helicopter 48th Annual Forum, Washington, D.C., 1992.

[17] Dadone, L.U., ìDesign and Analytical Study of a Rotor Airfoil,î NASA Contractor Report 2988, May 1978.

[18] Tapia, F., Sankar, L., Schrage, D., ìAn Inverse Aerodynamic Design Method for Rotor Blades,î *Journal of the American Helicopter Society*, Vol. 42, Number 4, October 1997.

[19] Liu, J., Paisley, D. J., Hirsh, J., ìTiltrotor Aerodynamic Blade Design by Numerical Optimization Method,î Proceedings of the American Helicopter Society 46th Annual Forum, Washington DC, May 21-23, 1990.

[20] Alexander, H. R., Hengen, L. M., Weiberg, J. A., ìAeroelastic Stability Characteristics of a V/STOL Tilt-Rotor Aircraft with Hingeless Blades: Correlation of Analysis and Test,î Stand-by Paper for the Dynamics Session of the 30th Annual Forum of the American Helicopter Society, May, 1974.

[21] Smith, K., Alexander, H., Maisel, M., ìDesign Aspects of the XV-15 Advanced Technology Blade Program,î Proceedings of the American Helicopter Society Annual Forum, Washington DC, May 15-17, 1985.

[22] Ganguli, G., Chopra, I., ìAeroelastic Optimization of a Helicopter Rotor with Composite tailoring and Advanced Tips,î Fifth Workshop on Dynamics & Aeroelastic Stability Modeling of Rotorcraft Systems, Rensselaer Polytechnic Inst., Troy NY, October, 1993.

[23] Tarzanin, F., ìBoeing Rotorcraft Experience with Rotor Design and Optimization,î AIAA-98-4733, 1998.

[24] Walsh, J., Young, K., Pritchard, J., Adelman, H., Mantay, ìIntegrated Aerodynamic/Dynamic/Structural Optimization of Helicopter Rotor Blades Using Multilevel Decomposition,î NASA TP-3465, 1995.

[25] Derham, R. C., Hagood, N. W., ìRotor Design Using Smart Materials to Actively Twist Blades,î Proceedings of the American Helicopter Society 50th Annual Forum, Washington DC, June 4-6, 1996.

[26] Kreisselmeier, G., Steinhauser, R., ìSystematic Control Design by Optimizing A Vector Performance Function,î Proceedings of IFAC Symposium on Computer Aided Design of Control Systems, Zurich, Switzerland, 1979, pp 113-117.

[27] Orr, S. ìIntegrated Aerodynamic and Dynamic Optimization of Tiltrotor Wing and Rotor Systemsî, Ph.D. Dissertation, Rensselaer Polytechnic Institute, Troy, NY, 2004.

[28] Montgomery, D. C., *Design and Analysis of Experiments*, 5th Edition, John Wiley & Sons, 2001.

[29] Wilkerson, J.B., Schneider, J.J., Bartie, K.M., ì Technology Needs for High-Speed Rotorcraft (I),î NASA Contactor Report 177585, 1991.
[30] Orr, S., Hajela, P., ì Genetic Algorithm Based Collaborative Optimization of a Tiltrotor Configuration,î AIAA 2005-2283, 2005.